COBEM-2017-2908
DYNAMIC ANALYSIS OF THE FLUID FLOW OVER A WIND TURBINE BLADE

Renata Ferreira Martins Rocha
Aldemir Aparecido Cavalini Junior
João Marcelo Vedovoto
MFLab – Fluid Mechanics Laboratory, Federal University of Uberlandia, School of Mechanical Engineering, MG, Brazil
renatarocha@ufu.br; aacjunior@ufu.br; vedovoto@ufu.br

Abstract. *This work is devoted to the dynamic analysis of an incompressible fluid flow over a wind turbine blade using the AMR3D platform to perform the numerical simulation. AMR3D is a computational Fortran90 code used to accomplish computational simulations of incompressible flows. The LES approach (Large Eddy Simulation) is used to model the inherent flow turbulence and profile NACA 0012 is considered to design the blade.*

Keywords: *fluid dynamics, wind turbine blade, incompressible flow.*

1. INTRODUCTION

Fluid dynamics is an important area to solve a lot of practical problems. One can quote aerodynamics, thermodynamics, hydraulics, and other areas which problems involve this subject. Fluid dynamic analyses are accomplished with experiments and theoretical methods. An important example of theoretical methods are the computational methods which are used to perform numerical solutions applied to fluid dynamics.

Mathematical model for fluid flows is established on balance equations of momentum, mass, and energy. When these equations are submitted to appropriate boundary and initial conditions they represent mathematically a particular problem. The analytical solution of these equations are only possible to very simple flows. Numerical methods are used for analyse real problems.

The laminar flows' models are very simple because the Navier-Stokes' equations and that of balance of mass and energy are resolved. But most of the flows that occur in nature and in the industry environment are turbulent, and these are very complex and should be used turbulence mathematical models. Turbulence models rely on statistics variables because they are very chaotic so statistics variables are used to represent turbulent flows.

The Immersed Boundary Method (IBM) is adopted to model the proposed problem. The results presented in this work represent the flow behaviour and the geometry isn't the entire wind turbine, but a single blade.

2. DIFFERENTIAL MATHEMATICAL MODELING

There are presented the differential equations to solve the dynamic behaviour of the fluid flow. The Eq. (1) represents the mass balance considering incompressible flow in Cartesian coordinates and using indicial notation.

$$\frac{\partial u_j}{\partial x_j} = 0, \ j = 1, 2, 3, \tag{1}$$

where x_j are the coordinates x, y and z, respectively of the referential of the fluid domain and u_j is the velocity of the fluid in j direction. The Eq. (2) represents the momentum balance considering Newtonian fluid and constant specific mass wrote in divergent form, in Cartesian coordinates and indicial notation.

$$\frac{\partial u_i}{\partial t} + \frac{\partial (u_i u_j)}{\partial x_j} = -\frac{1}{\rho_f}\frac{\partial P}{\partial x_i} + \frac{\partial}{\partial x_i}\left[\nu\left(\frac{\partial u_i}{\partial x_j} + \frac{\partial u_j}{\partial x_i}\right)\right], \tag{2}$$

where i and j=1,2,3, P is the pressure and t is the temporal variable. The Eqs. (1) and (2) are enough to solve the dynamic behaviour of the fluid flow, but solve all scales of the flow is not computationally viable.

With this, were used LES methodology to solve the large scales and the interactions between the large and the small scales. To use LES methodology is necessary to filter the Eqs. (1) and (2) two times, to get the transport's equations of the filtered velocities that corresponds to large scales that are solved. Applying in the Eqs. (1) and (2) the first filter $\overline{G}$ with characteristic length $\overline{\Delta}$ one obtains the Eqs. (3) and (4).

$$\frac{\partial \overline{u_j}}{\partial x_j} = 0, \tag{3}$$

$$\frac{\partial \overline{u_i}}{\partial t} + \frac{\partial (\overline{u_i u_j})}{\partial x_j} = -\frac{1}{\rho_f}\frac{\partial \overline{P}}{\partial x_i} + \frac{\partial}{\partial x_j}\left[\nu\left(\frac{\partial \overline{u_i}}{\partial x_j} + \frac{\partial \overline{u_j}}{\partial x_i}\right)\right], \tag{4}$$

where the top bar represents the filtering operator with the filter $\overline{G}$. Defining τ_{ij} as the tensor sub-mesh stress (or Reynolds stress) that can be written as shown in Eq. (5).

$$\tau_{ij} = \overline{u_i u_j} - \overline{u_i}\,\overline{u_j}. \tag{5}$$

The Eq. (4) can be written as shown in Eq. (6).

$$\frac{\partial \overline{u_i}}{\partial t} + \frac{\partial (\overline{u_i u_j})}{\partial x_j} = -\frac{1}{\rho_f}\frac{\partial \overline{P}}{\partial x_i} + \frac{\partial}{\partial x_j}\left[\nu\left(\frac{\partial \overline{u_i}}{\partial x_j} + \frac{\partial \overline{u_j}}{\partial x_i}\right) - \tau_{ij}\right]. \tag{6}$$

The Eq. (5) models the interaction between the resolved scales and the ones that must be modeled and depends on the expression $\overline{u_i u_j}$ that is not solved in the Eqs. (3) and (6). The second filter $\overline{\overline{G}}$ has characteristic length $\overline{\overline{\Delta}} > \overline{\Delta}$ should be applied in the Eq. (4), to obtain Eq. (7).

$$\frac{\partial \overline{\overline{u_i}}}{\partial t} + \frac{\partial (\overline{\overline{u_i u_j}})}{\partial x_j} = -\frac{1}{\rho_f}\frac{\partial \overline{\overline{P}}}{\partial x_i} + \frac{\partial}{\partial x_j}\left[\nu\left(\frac{\partial \overline{\overline{u_i}}}{\partial x_j} + \frac{\partial \overline{\overline{u_j}}}{\partial x_i}\right)\right]. \tag{7}$$

Defining the tensor of the stresses related to the second filter (also called sub-test tensor) as shown in Eq. (8).

$$T_{ij} = \overline{\overline{u_i u_j}} - \overline{\overline{u_i}}\,\overline{\overline{u_j}}. \tag{8}$$

So the Eq. (7) can be written as shown in Eq. (9).

$$\frac{\partial \overline{\overline{u_i}}}{\partial t} + \frac{\partial (\overline{\overline{u_i}}\,\overline{\overline{u_j}})}{\partial x_j} = -\frac{1}{\rho_f}\frac{\partial \overline{\overline{P}}}{\partial x_i} + \frac{\partial}{\partial x_j}\left[\nu\left(\frac{\partial \overline{\overline{u_i}}}{\partial x_j} + \frac{\partial \overline{\overline{u_j}}}{\partial x_i}\right) - T_{ij}\right]. \tag{9}$$

Applying in the Eq. (6) the filter $\overline{\overline{G}}$, one obtains Eq. (10).

$$\frac{\partial \overline{\overline{u_i}}}{\partial t}+\frac{\partial(\overline{\overline{u_i u_j}})}{\partial x_j}=-\frac{1}{\rho_f}\frac{\partial \overline{\overline{P}}}{\partial x_i}+\frac{\partial}{\partial x_j}\left[\nu\left(\frac{\partial \overline{\overline{u_i}}}{\partial x_j}+\frac{\partial \overline{\overline{u_j}}}{\partial x_i}\right)-\overline{\overline{\tau_{ij}}}\right]. \tag{10}$$

Subtracting the Eq. (10) from Eq. (9), one defines the Leonard's tensor as shown in Eq. (11).

$$L_{ij}=\overline{\overline{u_i u_j}}-\overline{\overline{u_i}}\,\overline{\overline{u_j}}=T_{ij}-\overline{\overline{\tau_{ij}}}. \tag{11}$$

According to Lesieur (2008) the most simple way to model the Reynolds tensor (Eq. (5)) is supposing the turbulent viscosity proposed by Boussinesq with the deviating part of the tensor can be modeled as a function of a turbulent viscosity and the filtered deformation rate tensor (using the filter $\overline{G}$) as shown in Eq. (12).

$$\tau_{ij}-\frac{1}{3}\delta_{ij}\tau_{kk}=-2\nu_t\overline{S_{ij}}, \tag{12}$$

where ν_t is the turbulent cinematic viscosity, δ_{ij} is the Kronecker's delta and $\overline{S_{ij}}$ is the deformation rate tensor written as a function of the filtered velocities as shown in Eq. (13).

$$\overline{S_{ij}}=\frac{1}{2}\left(\frac{\partial \overline{u_i}}{\partial x_j}+\frac{\partial \overline{u_j}}{\partial x_i}\right). \tag{13}$$

The turbulent viscosity can be modeled as in Eq. (14).

$$\nu_t=c(\vec{x},t)\overline{\Delta}^2\,|\overline{S}|, \tag{14}$$

where $|\overline{S}|=\sqrt{2\overline{S}\overline{S}}$. So, it's possible writing the Eq. (12) as shown in Eq. (15).

$$\tau_{ij}-\frac{1}{3}\delta_{ij}\tau_{kk}=-2c(\vec{x},t)\overline{\Delta}^2\,|\overline{S}|\,\overline{S_{ij}}. \tag{15}$$

The deviating part of the sub-test tensor (Eq. (8)) can be modelled as shown in Eq. (16).

$$T_{ij}-\frac{1}{3}\delta_{ij}T_{kk}=-2c(\vec{x},t)\overline{\overline{\Delta}}^2\,|\overline{S}|\,\overline{\overline{S_{ij}}}. \tag{16}$$

Filtering the Eq. (15) using the filter $\overline{\overline{G}}$, one obtains Eq. (17).

$$\overline{\overline{\tau_{ij}}}-\frac{1}{3}\delta_{ij}\overline{\overline{\tau_{kk}}}=-2c(\vec{x},t)\overline{\overline{\overline{\Delta}^2\,|\overline{S}|\,\overline{S_{ij}}}}. \tag{17}$$

With the Eqs. (11), (12), (15) and (16) and doing mathematics manipulations, one obtains Eq. (18).

$$c(\vec{x},t)=-\frac{1}{2}\frac{L_{ij}M_{ij}}{M_{ij}M_{ij}}, \tag{18}$$

where $M_{ij}=\overline{\overline{\Delta}}^2\,|\overline{\overline{S}}|\,\overline{\overline{S_{ij}}}-\overline{\overline{\overline{\Delta}^2\,|\overline{S}|\,\overline{S_{ij}}}}$. Replacing the Eq. (12) and the Eq. (13) in the Eq. (4), one obtains Eq. (19).

$$\frac{\partial \overline{u_i}}{\partial t}+\frac{\partial(\overline{u_i}\,\overline{u_j})}{\partial x_j}=-\frac{1}{\rho_f}\frac{\partial \overline{P}}{\partial x_i}-\frac{1}{3}\frac{\partial \delta_{ij}\tau_{kk}}{\partial x_i}+\frac{\partial}{\partial x_j}\left[\nu\left(\frac{\partial \overline{u_i}}{\partial x_j}+\frac{\partial \overline{u_j}}{\partial x_i}\right)+\nu_t\left(\frac{\partial \overline{u_i}}{\partial x_j}+\frac{\partial \overline{u_j}}{\partial x_i}\right)\right]. \tag{19}$$

The top bar of the sub-mesh tensor can be incorporated in pressure as shown in Eq. (20).

$$\overline{p}=\overline{P}+\frac{1}{3}\rho_f\delta_{ij}\tau_{kk}, \tag{20}$$

where $\overline{p}$ is the modified pressure. Replacing the Eq. (20) in the Eq. (19), one obtains Eq. (21).

$$\frac{\partial \overline{u_i}}{\partial t}+\frac{\partial(\overline{u_i}\,\overline{u_j})}{\partial x_j}=-\frac{1}{\rho_f}\frac{\partial \overline{p}}{\partial x_i}+\frac{\partial}{\partial x_j}\left[\nu_{ef}\left(\frac{\partial \overline{u_i}}{\partial x_j}+\frac{\partial \overline{u_j}}{\partial x_i}\right)\right], \tag{21}$$

where ν_{ef} is the effective cinematic viscosity calculated as the sum of the molecular cinematic viscosity with the turbulent cinematic viscosity, ν_t. The turbulent viscosity is obtained through the Eq. (14) that comes from the model of Germano et al. (1991). Therefore the Eq. (21) is the one that will be numerically solved.

3. RESULTS AND DISCUSSION

Figure 1 shows the blade geometry (NACA 0012 profile) which has a 50 cm span and 20 cm chord. The boundary condition is clamped-free and just the surface was considered. The fluid domain has 4 m x 0.8 m x 0.8 m in X (principal direction of the flow), Y and Z directions, respectively. The fluid domain's discretization has 7 physical levels of refinement of the mesh as shown in Fig. 2. The base mesh has 20 cells x 4 cells x 4 cells in X, Y and Z directions, respectively, from which it has the subsequent mesh refinements.

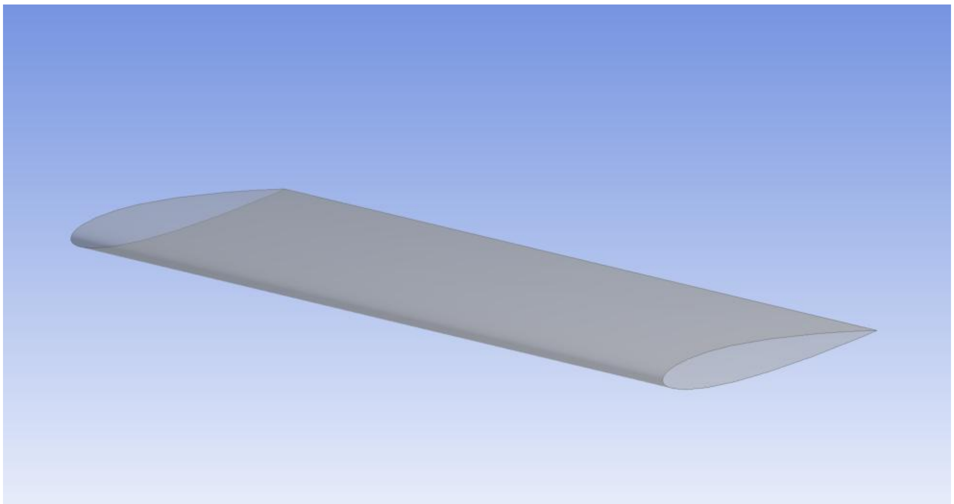

Figure 1. Blade surface which has 50 cm span and 20 cm chord

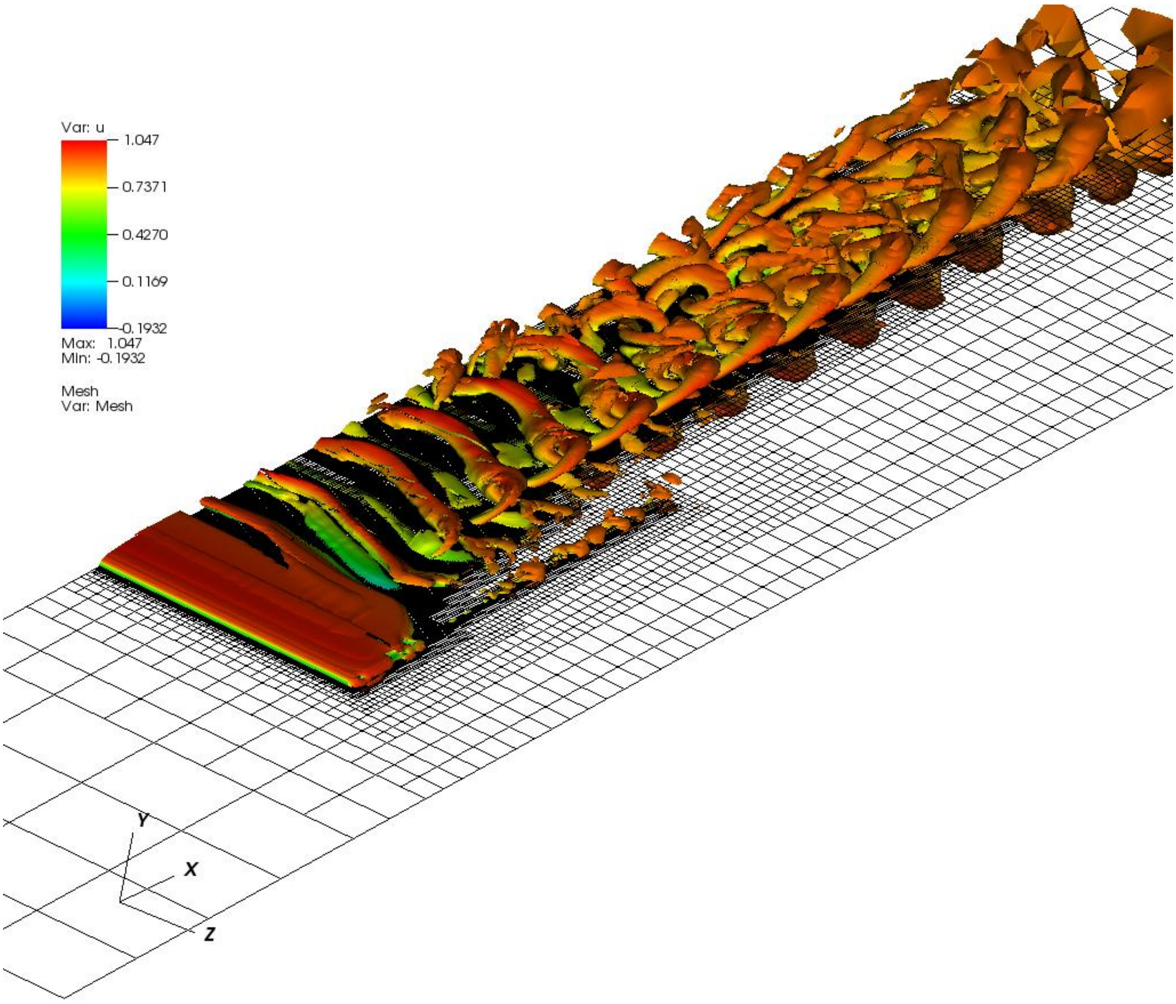

Figure 2. Visualization of the mesh and its refinements and the tridimensional flow over a blade using the value of Q criteria of 0.1 colored by the velocity in the X direction (velocity u) at the time of 40 s

The calculation of the case was divided in 5 sub-domains using a total of 4,063,842 computational volumes. The boundary conditions are the Dirichlet's boundary condition (imposed velocity) at the domain's entrance using the value of u=1.0 m/s, which corresponds to the flow's principal direction.

The fluid's specific mass is 1.0 kg/m^3 and the dynamic viscosity is $1.82x10^{-5}$ Ns/m^2, therefore it was used the air as the fluid. Figure 2 shows the visualization of the Q criteria (tridimentional vortex) colored by u velocity (velocity in the X direction) and the simulation time is 40 s.

This flow is dynamically characterized by a value of Reynolds number of $2.747x10^4$. According to literature this type of flow usually becomes turbulent at Reynolds number of $4x10^3$. Therefore, the flow safely transitions to turbulence as one can see at Fig. 2 instabilities next to the domain's exit.

Figure 3 shows with more details Fig. 2 to evince the instabilities formed after the flow passes through the blade tip. This phenomenon is named by wing tip vortex and characterizes the vortex formed by the wing tip.

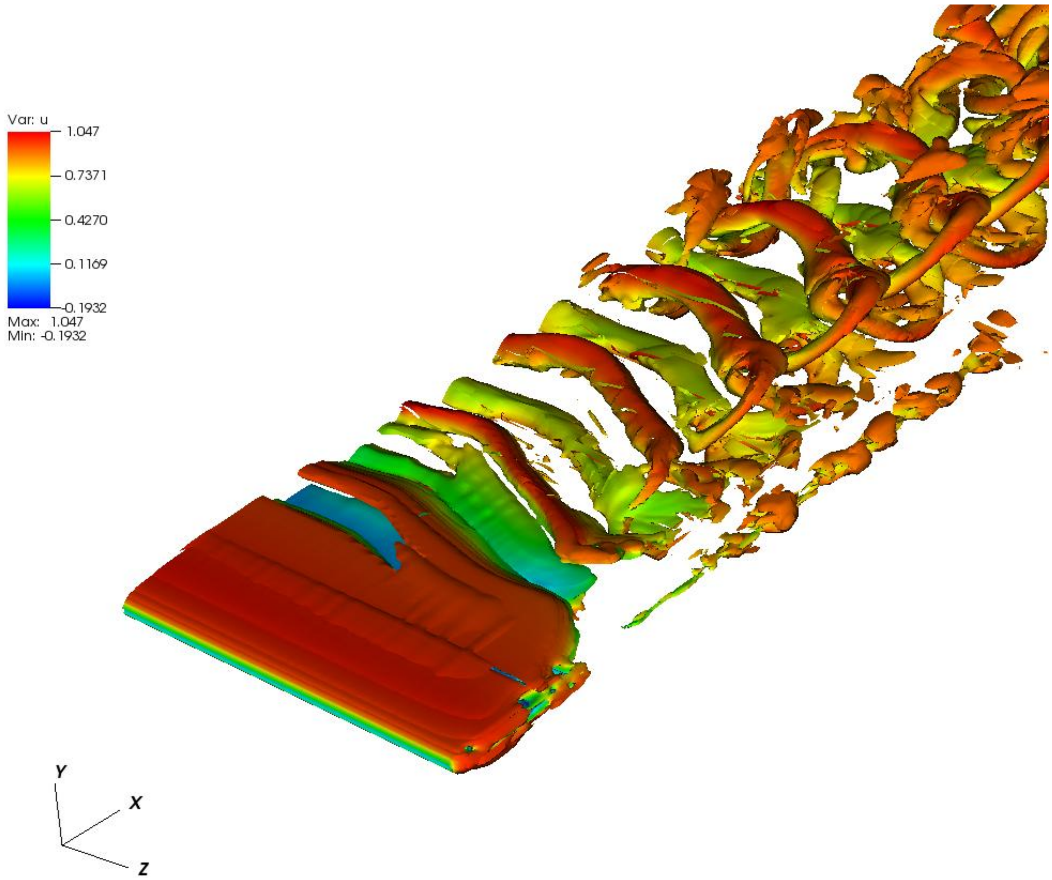

Figure 3. Visualization of the instabilities formed by the blade tip

The recommendations for futures works are for the purpose to compare the obtained results with literature and possibly to emphasize the detected phenomenon analysis at the blade tip.

4. ACKNOWLEDGEMENTS

The authors are thankful to the Brazilian Research Agencies FAPEMIG and CNPq (INCT-EIE) and to CAPES and Petrobras S.A. for the financial support provided for this research.

5. REFERENCES

Andrade, J. R., 2015. *Immersed boundary method for thin bodies: implementation and validation.* Master dissertation, Federal University of Uberlandia, Uberlandia.

Germano, M., Piomelli, U., Moin, P., Cabot, W. H., 1991. “A dynamic subgrid-scale eddy viscosity model. Physics of fluids A”. <http://scitation.aip.org/content/aip/journal/pofa/3/7/10.1063/1.857955>.

Granger, Robert A., *Fluid Mechanics*, Dover Publications, inc., New York - 1995.

Lesieur, M., 2008. *Turbulence in fluids*. Springer, 4th.

Lixing, Zhou, *Theory and Numerical Modeling of Turbulent Gas-Particle Flows and Combustion*, 1993, Science Press - China.

McDonald, A. T., R. W., Fox, *Introduction to Fluid Mechanics*, LTC - 1998.

Ribeiro Neto, H., 2016. *Mathematical modeling for the fluid structure interaction coupling incompressible flows and Timoshenko beams.* Master dissertation, Federal University of Uberlandia, Uberlandia.

Sotiropoulos, F., Yang, X., *Immersed boundary methods for simulating fluid-structure interaction. Progress in Aerospace Sciences*, Pergamon, 2014.

White, F. M., 1998. *Fluid mechanics.*New York, USA. McGraw-Hill, 4th.

6. RESPONSIBILITY NOTICE

The authors are the only responsible for the printed material included in this paper.